On thin shallow elastic shells over polygonal bases

Autor(en): **Walkinshaw, D.S. / Riley, G.E. / Siddall, J.N.**

Objekttyp: **Article**

Zeitschrift: **IABSE publications = Mémoires AIPC = IVBH Abhandlungen**

Band (Jahr): **28 (1968)**

PDF erstellt am: **16.08.2024**

Persistenter Link: https://doi.org/10.5169/seals-22176

Nutzungsbedingungen

Die ETH-Bibliothek ist Anbieterin der digitalisierten Zeitschriften. Sie besitzt keine Urheberrechte an den Inhalten der Zeitschriften. Die Rechte liegen in der Regel bei den Herausgebern.
Die auf der Plattform e-periodica veröffentlichten Dokumente stehen für nicht-kommerzielle Zwecke in Lehre und Forschung sowie für die private Nutzung frei zur Verfügung. Einzelne Dateien oder Ausdrucke aus diesem Angebot können zusammen mit diesen Nutzungsbedingungen und den korrekten Herkunftsbezeichnungen weitergegeben werden.
Das Veröffentlichen von Bildern in Print- und Online-Publikationen ist nur mit vorheriger Genehmigung der Rechteinhaber erlaubt. Die systematische Speicherung von Teilen des elektronischen Angebots auf anderen Servern bedarf ebenfalls des schriftlichen Einverständnisses der Rechteinhaber.

Haftungsausschluss

Alle Angaben erfolgen ohne Gewähr für Vollständigkeit oder Richtigkeit. Es wird keine Haftung übernommen für Schäden durch die Verwendung von Informationen aus diesem Online-Angebot oder durch das Fehlen von Informationen. Dies gilt auch für Inhalte Dritter, die über dieses Angebot zugänglich sind.

Ein Dienst der *ETH-Bibliothek*
ETH Zürich, Rämistrasse 101, 8092 Zürich, Schweiz, www.library.ethz.ch

http://www.e-periodica.ch

On Thin Shallow Elastic Shells over Polygonal Bases

Des coques minces élastiques à courbure faible, ayant une base polygonale

Über dünne, flache, elastische Schalen vieleckigen Grundrisses

D. S. WALKINSHAW
Defence Research Board, Ralston, Alberta, Canada

G. E. RILEY
Professional Engineer, Province of Ontario, Canada

J. N. SIDDALL
Associate Professor of Mechanical Engineering, McMaster University, Hamilton, Ontario, Canada

G. AE. ORAVAS
Professor of Engineering Mechanics, McMaster University, Hamilton, Ontario, Canada

Introduction

This paper demonstrates the applicability of the approximate theoretical solution given by ORAVAS in 1957 [1][1]) for shallow thin calotte shells of spherical middle surface subjected to isothermal deformations by uniform normal pressures.

Although spherical calotte shells have been constructed in practice, as far as is known any analytical solution used in their design neglected the shell's transverse bending stiffness. Such momentless analyses introduce errors in the solution, particularily near the shell's boundary where transverse bending is important. The extent of penetration of this transverse bending zone towards the shell's apex depends upon the shell's thickness, middle surface curvature, boundary periodicity and loading.

The theoretical solution is based on a collocation procedure introduced for plates by TÖLKE in 1934 [2] by means of which prescribed boundary conditions are satisfied at discrete boundary points. In this method, derived from the general theory given by MUSHTARI in 1938 [3] and VLASOV in 1949 [4], the transverse shear deformation of the shell is neglected in comparison with its transverse bending and extensional surface deformation.

---

[1]) Numbers in brackets designate references at end of paper.

Sectional resultants obtained both theoretically and experimentally for a spherical shell enclosing an hexagonal base are graphically depicted for various radial lines of the characteristic segment of the shell.

Theoretical sectional resultants are also depicted for a similar spherical shell enclosing a triangular base.

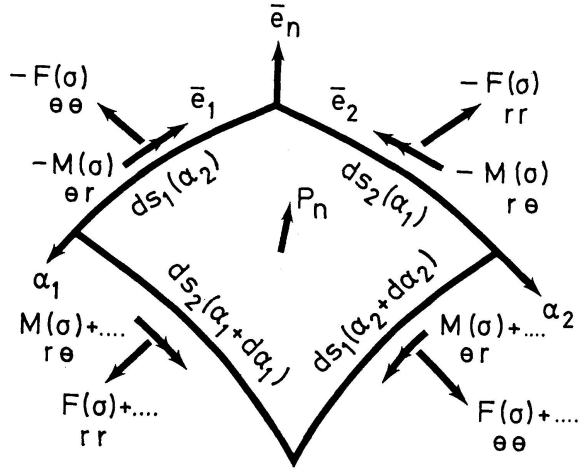

Fig. 1. Vector diagram of shell element showing sectional resultants of stress.

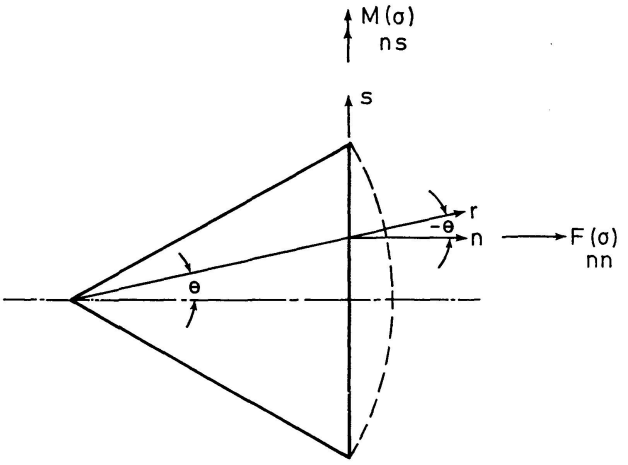

Fig. 2. Vector diagram showing relation of boundary coordinates n, s to shell interior coordinates r, θ.

Formulation of the Theoretical Solution

The two fundamental fourth order differential equations for thin shallow shells subjected to isothermal deformation by uniform normal loading given by MUSHTARI and VLASOV are

$$\begin{aligned} D\nabla^4 u_n + \frac{1}{R}\nabla^2 F &= p_n, \\ \nabla^4 F - \frac{Eh}{R}\nabla^2 u_n &= 0, \end{aligned} \tag{1}$$

where
u_n normal displacement
F stress function
p_n load intensity component per unit area normal to middle surface of shell
h constant shell thickness
E YOUNG's modulus of elasticity
R radius of curvature of middle surface of spherical shell
$D = E h^3/12(1-\nu^2) \equiv$ flexural rigidity of shell
$\nabla^2 \equiv \frac{d}{d\bar{r}_0}\frac{d}{d\bar{r}_0} \equiv \frac{\partial}{\partial r^2}+\frac{1}{r}\frac{\partial}{\partial r}+\frac{1}{r^2}\frac{\partial^2}{\partial\theta^2}$
$\nabla^4 \equiv \nabla^2\nabla^2$
ν POISSON's ratio
$\bar{r}_0$ radius vector to middle surface of shell
r radial parametric coordinate of shell
θ circumferential parametric coordinate of shell

MARGUERRE gave similar shallow shell equations in 1939 [5].

The solution of equations (1) under certain restrictions can be reduced to the solution of three differential equations

$$\begin{aligned} \nabla^2[\nabla^2 - i\lambda^2]V_0 &= \frac{p_n}{D}, \\ [\nabla^2 - i\lambda^2]\nabla^2 V_1 &= \nabla^2 V_1 = 0, \\ \nabla^2 V_2 - i\lambda^2 V_2 &= 0, \end{aligned} \tag{2}$$

where

$$\begin{aligned} V &= u_n + i\omega F = V_0 + V_1 + V_2, \\ \omega &= \sqrt{12(1-\nu^2)}/Eh^2, \\ \lambda^2 &= \sqrt{12(1-\nu^2)}/Rh \end{aligned}$$

and V_0, V_1 and V_2 represent three linearly independent solutions.

Solution of equations (2) yields the approximate normal displacement u_n and stress function F for a spherical shell of k-tuple symmetry. Since the shells which were investigated possessed no inner boundaries terms containing $\ker_n(x)$, $\mathrm{kei}_n(x)$ and r^{-n} are omitted from the solution because of their singular nature at the origin. Finally the solution becomes

$$\begin{aligned} u_n &= \frac{p_n R^2}{Eh} + A_0^1 \operatorname{ber}_0(\lambda r) + A_0^2 \operatorname{bei}_0(\lambda r) + E_0^1 \\ &\quad + \sum_{n=1}^{\infty}[A_{kn}^1 \operatorname{ber}_{kn}(\lambda r) + A_{kn}^2 \operatorname{bei}_{kn}(\lambda r) + C_{kn}^1 r^{kn}]\cos(kn\theta), \\ F &= \frac{p_n R r^2}{4} + \frac{1}{\omega}\{A_0^1 \operatorname{bei}_0(\lambda r) - A_0^2 \operatorname{ber}_0(\lambda r) + E_0^2 \\ &\quad + \sum_{n=1}^{\infty}[A_{kn}^1 \operatorname{bei}_{kn}(\lambda r) - A_{kn}^2 \operatorname{ber}_{kn}(\lambda r) + C_{kn}^2 r^{kn}]\cos(kn\theta)\}. \end{aligned} \tag{3}$$

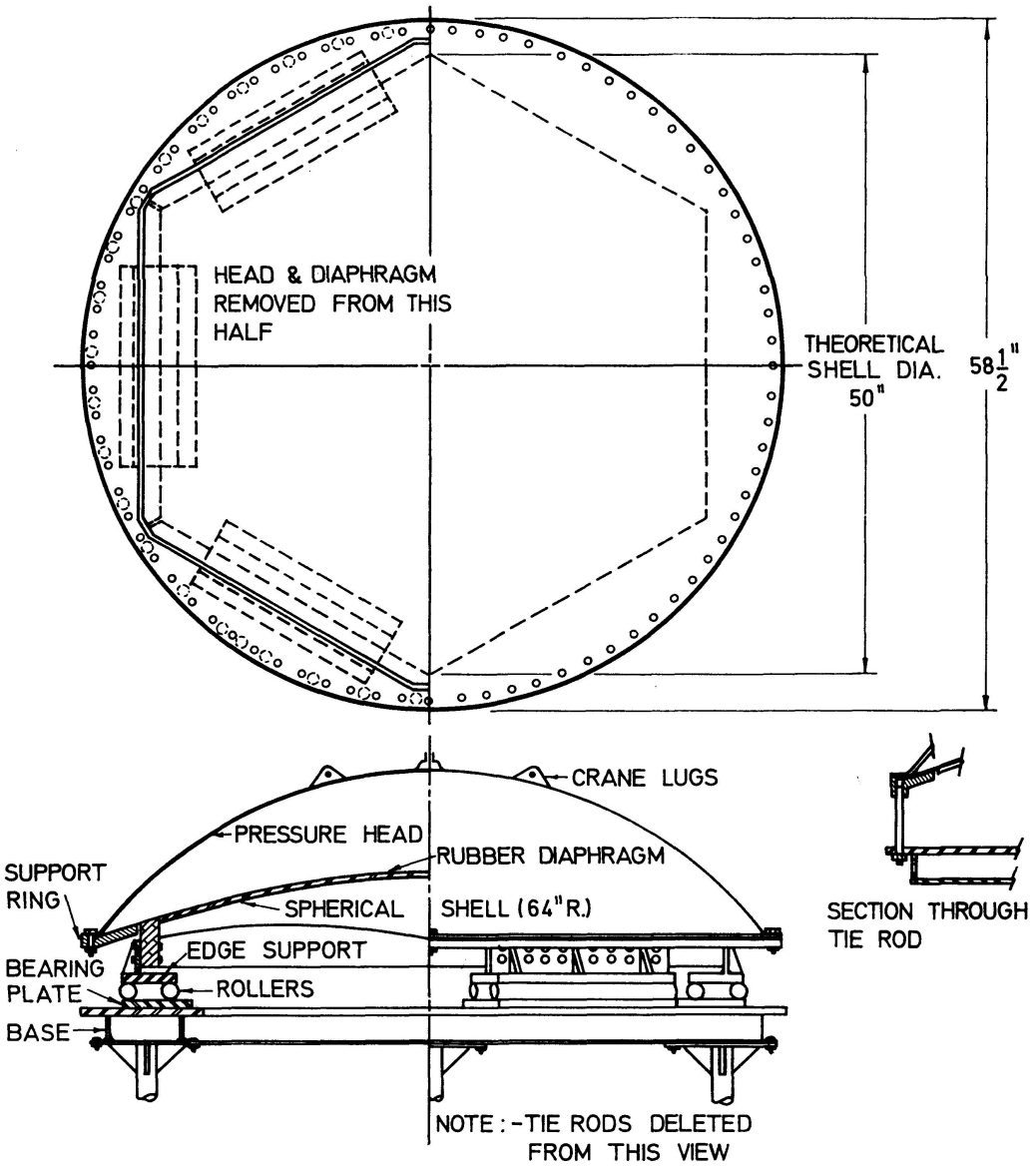

Fig. 3. Shell test assembly.

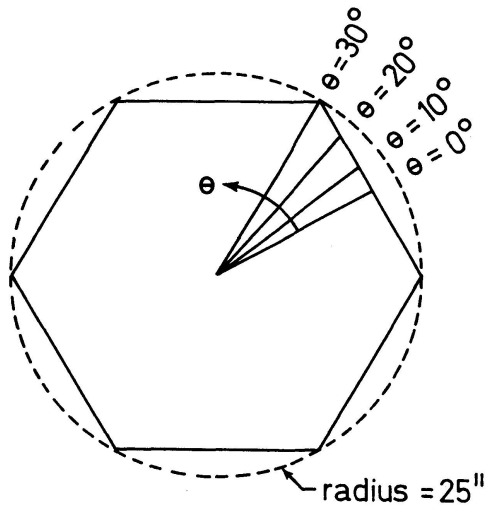

Fig. 4. Plan view of shell on hexagonal base showing location of radial lines for which sectional resultants of stress are calculated.

Sectional stress resultants and stress couples can be expressed in terms of the normal displacement and the stress function as

$$F_{\theta\theta}(\sigma) = \frac{\partial^2 F}{\partial r^2},$$

$$F_{rr}(\sigma) = \frac{1}{r}\frac{\partial F}{\partial r} + \frac{1}{r^2}\frac{\partial^2 F}{\partial \theta^2},$$

$$F_{r\theta}(\sigma) = F_{\theta r}(\sigma) = -\frac{\partial}{\partial r}\left(\frac{1}{r}\frac{\partial F}{\partial \theta}\right) \tag{4}$$

and

$$M_{r\theta}(\sigma) = -D\left[\frac{\partial^2 u_n}{\partial r^2} + \nu\left(\frac{1}{r^2}\frac{\partial^2 u_n}{\partial \theta^2} + \frac{1}{r}\frac{\partial u_n}{\partial r}\right)\right],$$

$$M_{\theta r}(\sigma) = D\left[\frac{1}{r^2}\frac{\partial^2 u_n}{\partial \theta^2} + \frac{1}{r}\frac{\partial u_n}{\partial r} + \nu\frac{\partial^2 u_n}{\partial r^2}\right],$$

$$M_{rr}(\sigma) = -M_{\theta\theta}(\sigma) = \frac{\mu h^3}{6}\left[\frac{\partial}{\partial r}\left(\frac{1}{r}\frac{\partial u_n}{\partial \theta}\right)\right].$$

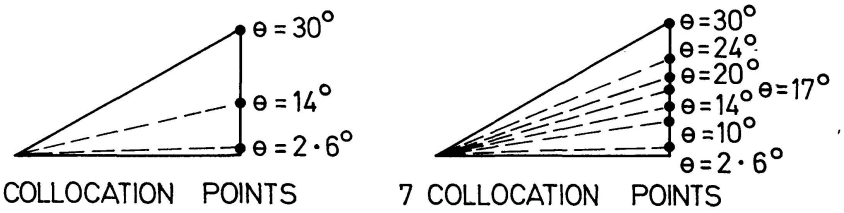

Fig. 5. Location of boundary collocation points for characteristic periodical segment of shell over hexagonal base.

The solution for the constants A_0^1, A_0^2, E_0^1, E_0^2, A_{kn}^1, A_{kn}^2, C_{kn}^1 and C_{kn}^2 in (3) is effected by employing TÖLKE's boundary collocation procedure which restricts idealized boundary conditions to be satisfied only at discrete boundary points instead of along the entire length of the boundary.

The boundary conditions relevant to the shallow calotte shells investigated are

a) Stress resultants normal to the boundary vanish:

$$F_{nn}(\sigma) = 0.$$

b) The boundary undergoes no rotation:

$$\delta\left(\frac{\partial u_n}{\partial n}\right) = 0.$$

c) The boundary undergoes no normal displacement:

$$u_n = 0. \tag{5}$$

d) The boundary is fully constrained and consequently undergoes no linear strain:

$$\epsilon_{ss} = 0.$$

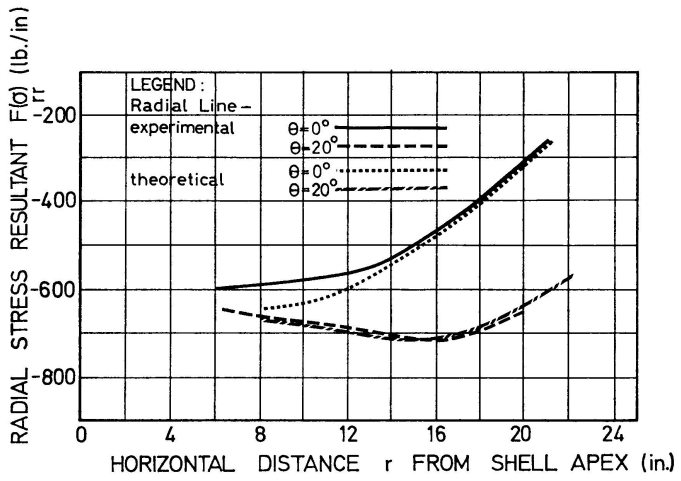

Fig. 6. Plot showing stress resultant "$F_{rr}(\sigma)$" for shell over hexagonal base obtained theoretically for three collocation points as well as experimentally.

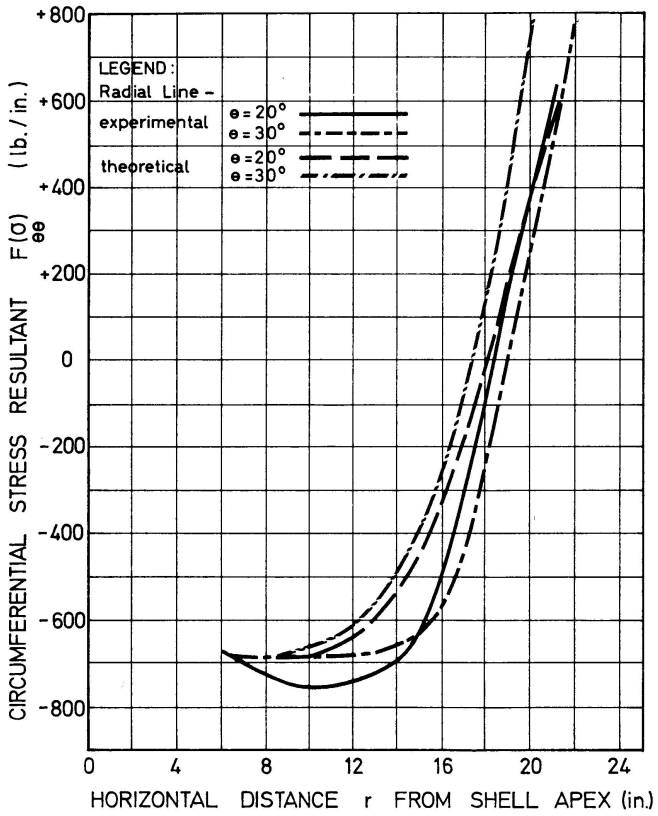

Fig. 7. Plot showing stress resultant "$F_{\theta\theta}(\sigma)$" for shell over hexagonal base obtained theoretically for three collocation points as well as experimentally.

e) The tangential stress couple vector vanishes along the boundary edge:

$$M_{ns} = 0.$$

Satisfaction of these boundary conditions, which can be expressed in terms of the normal displacement u_n and the stress function F, at points on the shell's boundary, results in a set of simultaneous equations whose solution yields the unknown constants in (3) allowing the calculation of the sectional resultants of stress.

Numerical Solution for a Spherical Shell Enclosing an Hexagonal Base

Experimental sectional resultants of stress were obtained for a spherical shell enclosing an hexagonal base subjected to isothermal deformation by a uniform normal load, by taking extensive strain measurements on the upper and lower surfaces of the shell. Sectional resultants were calculated theoretically for this shell using both three and seven boundary collocation points and satisfying the boundary conditions

$$\begin{aligned} F_{nn}(\sigma) &= -240 \text{ lb./in.}, \\ \delta\left(\frac{\partial u_n}{\partial n}\right) &= 0.00055 \text{ radians}, \\ u_n &= 0, \\ \epsilon_{ss} &= 0, \end{aligned}$$

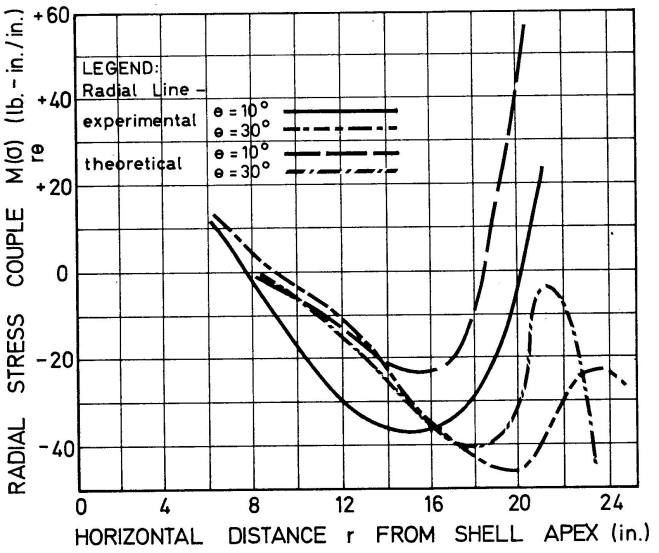

Fig. 8. Plot showing stress couple "$M_{r\theta}(\sigma)$" for shell over hexagonal base obtained theoretically for seven collocation points as well as experimentally.

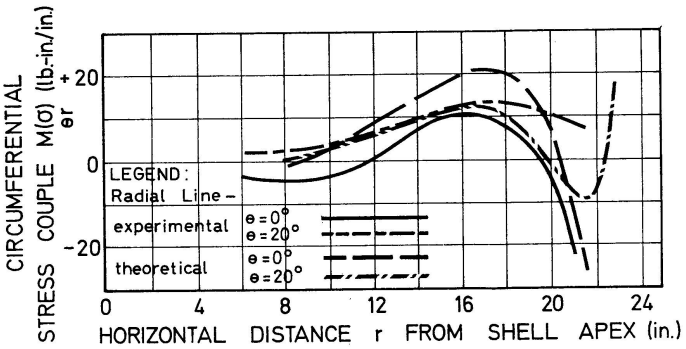

Fig. 9. Plot showing stress couple "$M_{\theta r}(\sigma)$" for shell over hexagonal base obtained theoretically for seven collocation points as well as experimentally.

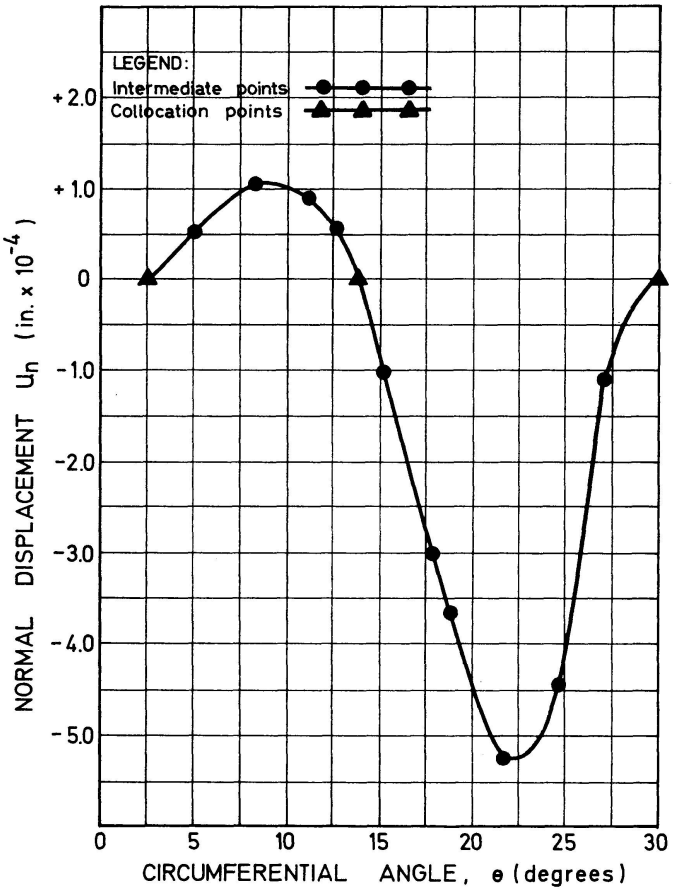

Fig. 10. Variation of "u_n" on the boundary of shell over hexagonal base for three collocation points.

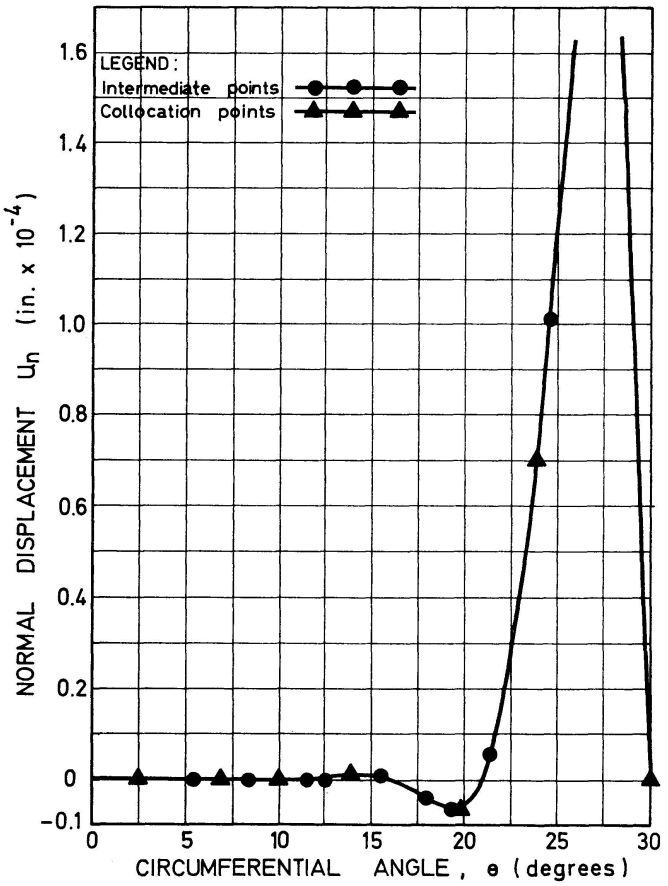

Fig. 11. Variation of "u_n" on the boundary of shell over hexagonal base for seven collocation points.

at each of the collocation points except at the shell's corners where the strain was not assumed to vanish.

Shell Parameters

$E = 10^7$ p.s.i. (aluminium),
$\nu = 0.33$,
$p_n = -20$ p.s.i.,
$R = 64$ in.,
$h = 0.375$ in.,
$k = 6$.

Numerical Solution for a Spherical Shell Enclosing a Triangular Base

A solution by the collocation technique is given for a spherical calotte shell enclosing a triangular base since shells of this type have been constructed in practice and no other theoretical solutions are known to exist.

The shell was assumed to be supported on a very narrow boundary diaphragm. Hence the boundary conditions

$$u_n = 0,$$
$$\epsilon_{ss} = 0,$$
$$M_{ns}(\sigma) = 0,$$
$$F_{nn}(\sigma) = 0,$$

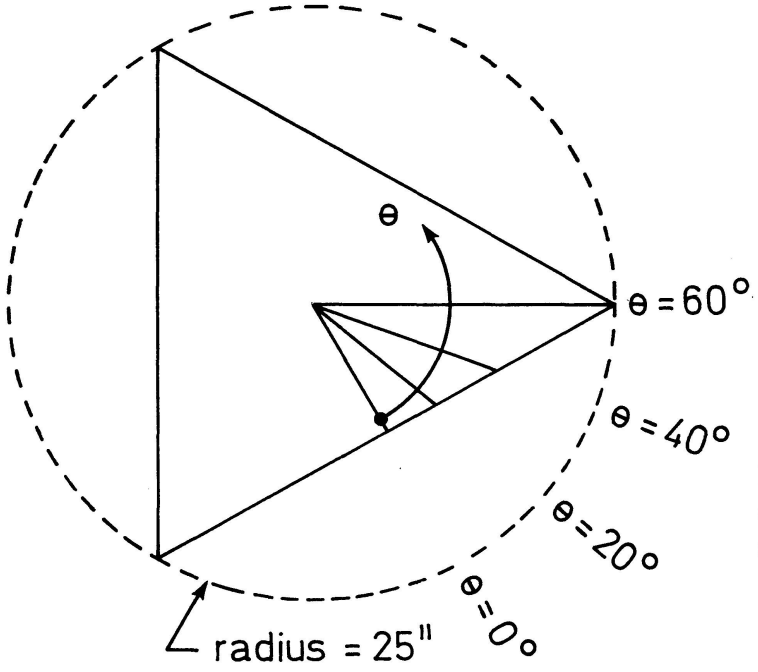

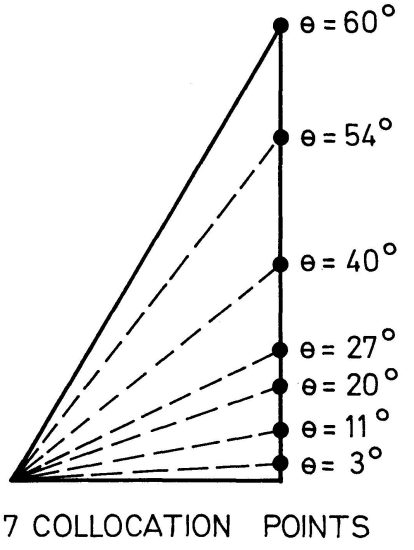

Fig. 13. Location of boundary collocation points for characteristic periodical segment of shell over triangular base.

Fig. 12. Plan view of shell over triangular base showing location of radial lines for which sectional resultants of stress are calculated.

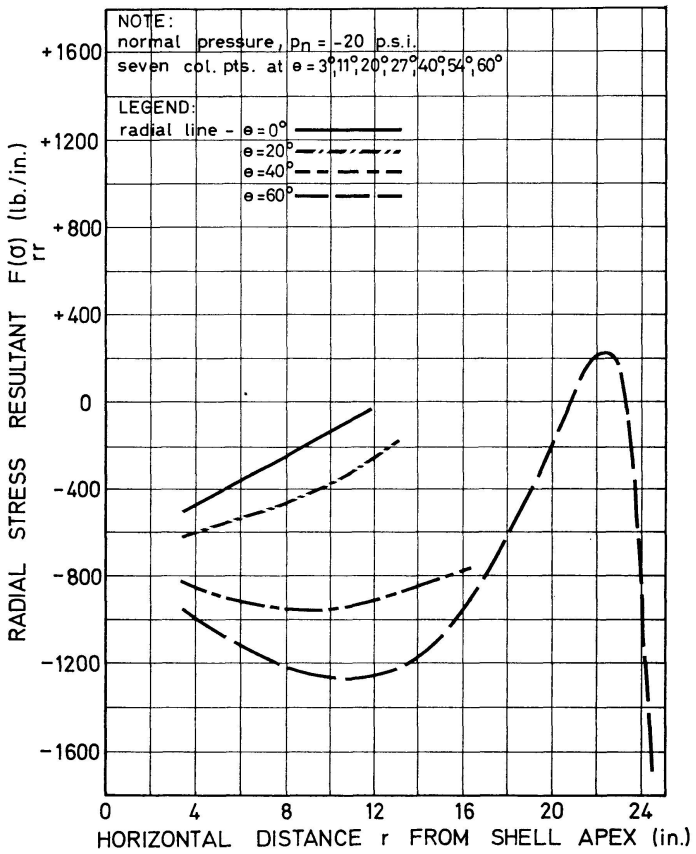

Fig. 14. Plot showing theoretical stress resultant "$F_{rr}(\sigma)$" for shell over triangular base.

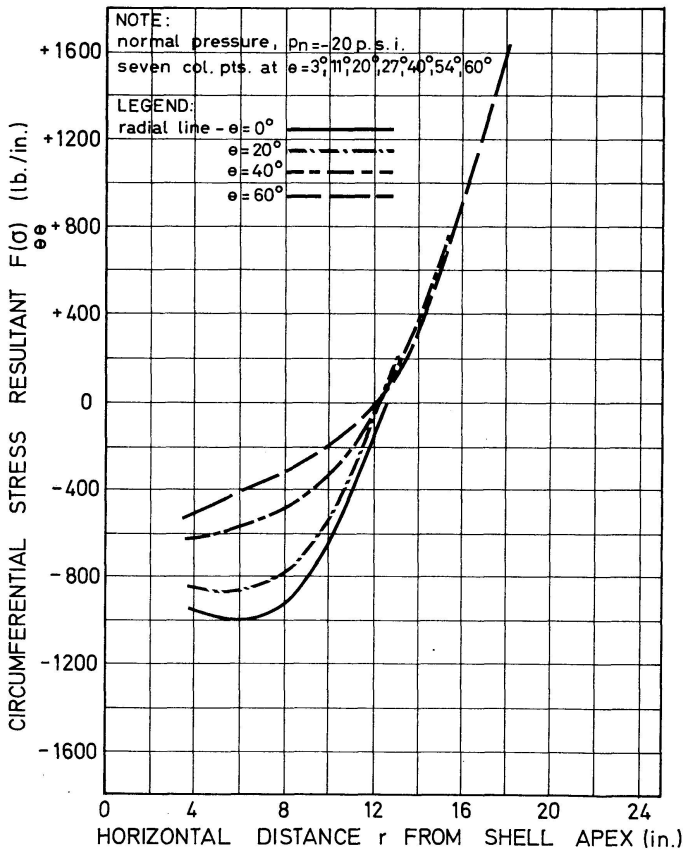

Fig. 15. Plot showing theoretical stress resultant "$F_{\theta\theta}(\sigma)$" for shell over triangular base.

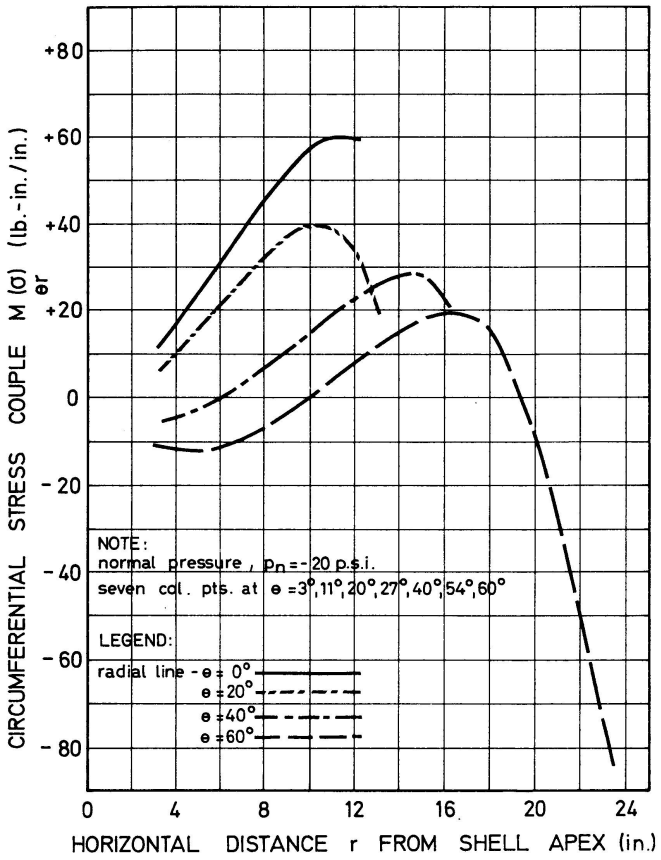

Fig. 16. Plot showing theoretical stress couple "$M_{r\theta}(\sigma)$" for shell over triangular base.

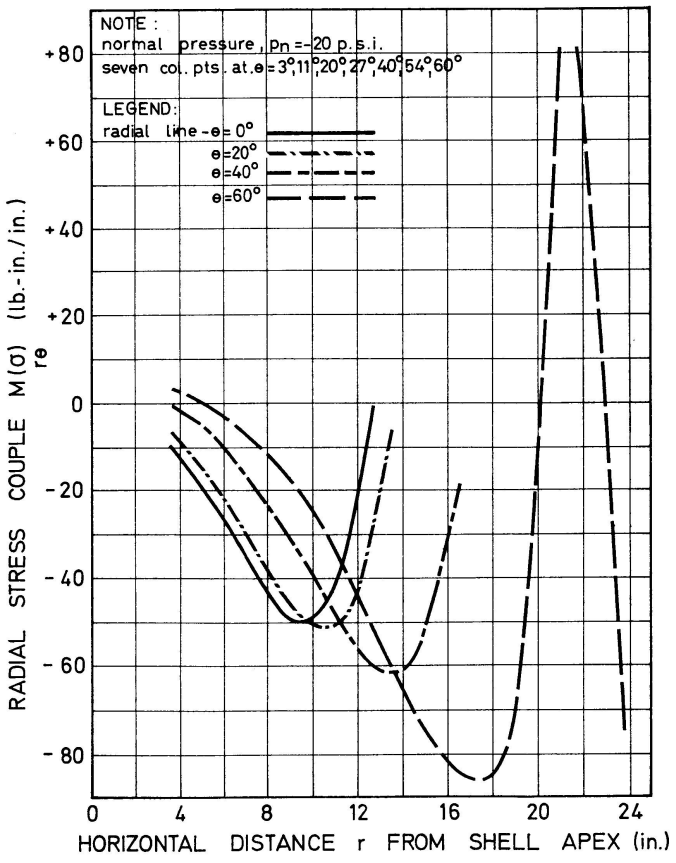

Fig. 17. Plot showing theoretical stress couple "$M_{\theta r}(\sigma)$" for shell over triangular base.

were satisfied at each of the collocation points except at the shell's corners where the normal boundary force $F_{nn}(\sigma)$ was not assumed to vanish.

Shell Parameters

$E = 10^7$ p.s.i.,
$\nu = 0.33$,
$p_n = -20$ p.s.i.,
$R = 64$ in.,
$h = 0.375$ in.,
$k = 3$.

Conclusions

The collocation technique satisfies idealized boundary conditions rigorously only at discrete boundary points. The number of boundary collocation points which will yield a solution satisfying these conditions over the entire shell boundary is not large. Theoretical solutions given by WALKINSHAW in 1965 [6] for a shell enclosing an hexagonal base employing three and seven collocation points on the boundary of the characteristic shell segment, agree reasonably well with experimental results obtained by RILEY in 1964 [7] for the same shell. Consequently for this calotte shell, three collocation points are sufficient to provide reliable solutions for practical design purposes. Obviously the minimum number of boundary collocation points providing reliable theoretical solutions increases as the circumferential periodicity of the calotte shell decreases.

The periodic polygonal boundary of a spherical shell introduces periodic perturbations in the rotationally symmetric solution emanating from the nonrotationally symmetric boundary. The extent of the penetration of these perturbations towards the shell's apex, where the rotationally symmetric solution associated with the zero order terms of the truncated series solution dominates, depends upon the degree by which the polygonal boundary deviates from the circular boundary of the rotational spherical shell enclosing the polygonal shell.

The experimental shell used in testing exhibited certain unavoidable geometric imperfections, which did not satisfy the conditions of perfect periodicity in the configuration of the six shell segments assumed in the theoretical solution. The boundary members were not connected at their intersection points in order to simulate the boundary conditions imposed by the theoretical solution as closely as possible. The discontinuity of the boundary members created some stress concentrations at the corners of the shell, which partially account for greater discrepancies between the theoretical and experimental results in these regions.

The boundary conditions in the experimental shell which were not uniform

along the boundary members, did not strictly satisfy the homogeneous theoretical boundary conditions. This shortcoming necessitated an introduction of average corrections to the theoretical boundary conditions which neglected the variations of the boundary conditions along the boundary members.

The theoretical solution and the experimental results were as compatible as could be expected in view of these physical limitations in both the construction and boundary conditions of the shell structure. Therefore, the experimental results can merely serve as a good indication for the general nature of the structural comportment of the shell treated in the theoretical problem.

The higher order KELVIN Functions employed in this collocative solution in the form of a truncated series were evaluated by means of the Backward Recurrence Technique, devised by J. C. P. MILLER and outlined in detail by T. E. MICHELS in 1964, using McMaster University's I.B.M. 7040 computer and double-precision procedure with 17 figure accuracy.

It was established that the number and location of the collocation points used are not of the paramount significance to the practical reliability of the results as was initially believed. The discrete satisfaction of boundary conditions in the collocative solution tends to accumulate larger magnitude errors in the results near the corners of the polygonal calotte shell and, therefore, it is to be expected that the collocative solution tends to deviate more from the actual solution in the neighbourhood of the corners of the shell than in the remaining region of the shell. It is considered that seven boundary collocation points provide a reliable practical solution for the calotte shell with as little as triple periodicity.

An Appendix has been given for various quantities in the theoretical solution, which correct all the misprints in the same expressions given by ORAVAS in 1957.

Appendix

Boundary conditions (5-a) to (5-e) can be expressed in terms of the normal displacement u_n and stress function F as:

$$
\begin{aligned}
&A_0^1\psi_1 + A_0^2\psi_2 + \sum_{n=1}^{\infty}[A_{kn}^1\psi_3 + A_{kn}^2\psi_4 + C_{kn}^2\psi_5] = \frac{-p_n R}{2},\\
&A_0^1\psi_6 + A_0^2\psi_7 + \sum_{n=1}^{\infty}[A_{kn}^1\psi_8 + A_{kn}^2\psi_9 + C_{kn}^1\psi_{10}] = 0,\\
&A_0^1\psi_{11} + A_0^2\psi_{12} + E_0^1 + \sum_{n=1}^{\infty}[A_{kn}^1\psi_{13} + A_{kn}^2\psi_{14} + C_{kn}^1\psi_{15}] = \frac{-p_n R^2}{E h}, \qquad \text{(A-1)}\\
&A_0^1\psi_{16} + A_0^2\psi_{17} + \sum_{n=1}^{\infty}[A_{kn}^1\psi_{18} + A_{kn}^2\psi_{19} + C_{kn}^2\psi_{20}] = -(1-\nu)\frac{p_n R}{2},\\
&A_0^1\psi_{21} + A_0^2\psi_{22} + \sum_{n=1}^{\infty}[A_{kn}^1\psi_{23} + A_{kn}^2\psi_{24} + C_{kn}^1\psi_{25}] = 0.
\end{aligned}
$$

The coefficients in equations (A-1) are:

$$\psi_1 = \frac{\lambda}{\omega\bar{r}}\mathrm{bei}_0'(\lambda\bar{r})\cos^2\bar{\theta} + \frac{\lambda^2}{\omega}\mathrm{bei}_0''(\lambda\bar{r})\sin^2\bar{\theta},$$

$$\psi_2 = -\frac{\lambda}{\omega\bar{r}}\mathrm{ber}_0'(\lambda\bar{r})\cos^2\bar{\theta} + \frac{\lambda^2}{\omega}\mathrm{ber}_0''(\lambda\bar{r})\sin^2\bar{\theta},$$

$$\psi_3 = \left\{\frac{\lambda}{\omega\bar{r}}\mathrm{bei}_{kn}'(\lambda\bar{r})\cos^2\bar{\theta} - \frac{(kn)^2}{\omega\bar{r}^2}\mathrm{bei}_{kn}(\lambda\bar{r})\cos^2\bar{\theta} + \frac{\lambda^2}{\omega}\mathrm{bei}_{kn}''(\lambda\bar{r})\sin^2\bar{\theta}\right\}\cos(kn\bar{\theta})$$
$$+ \left\{\frac{kn}{\omega\bar{r}^2}\mathrm{bei}_{kn}(\lambda\bar{r})\sin 2\bar{\theta} - kn\left(\frac{\lambda}{\omega\bar{r}}\right)\mathrm{bei}_{kn}'(\lambda\bar{r})\sin 2\bar{\theta}\right\}\sin(kn\bar{\theta}),$$

$$\psi_4 = \left\{-\frac{\lambda}{\omega\bar{r}}\mathrm{ber}_{kn}'(\lambda\bar{r})\cos^2\bar{\theta} + \frac{(kn)^2}{\omega\bar{r}^2}\mathrm{ber}_{kn}(\lambda\bar{r})\cos^2\bar{\theta}\right.$$
$$\left. - \frac{\lambda^2}{\omega}\mathrm{ber}_{kn}''(\lambda\bar{r})\sin^2\bar{\theta}\right\}\cos(kn\bar{\theta})$$
$$+ \left\{-\frac{kn}{\omega\bar{r}^2}\mathrm{ber}_{kn}(\lambda\bar{r}) + \frac{\lambda kn}{\omega\bar{r}}\mathrm{ber}_{kn}'(\lambda\bar{r})\right\}\sin 2\bar{\theta}\sin(kn\bar{\theta}),$$

$$\psi_5 = \frac{kn}{\omega}(kn-1)\bar{r}^{kn-2}[(\sin^2\bar{\theta} - \cos^2\bar{\theta})\cos(kn\bar{\theta}) - \sin 2\bar{\theta}\sin(kn\bar{\theta})],$$

$$\psi_6 = -\lambda\,\mathrm{ber}_0'(\lambda\bar{r})\cos\bar{\theta},$$

$$\psi_7 = -\lambda\,\mathrm{bei}_0'(\lambda\bar{r})\cos\bar{\theta},$$

$$\psi_8 = -\left[\frac{kn}{\bar{r}}\mathrm{ber}_{kn}(\lambda\bar{r})\sin\bar{\theta}\right]\sin(kn\bar{\theta}) - [\lambda\,\mathrm{ber}_{kn}'(\lambda\bar{r})\cos\bar{\theta}]\cos(kn\bar{\theta}),$$

$$\psi_9 = -\left[\frac{kn}{\bar{r}}\mathrm{bei}_{kn}(\lambda\bar{r})\sin\bar{\theta}\right]\sin(kn\bar{\theta}) - [\lambda\,\mathrm{bei}_{kn}'(\lambda\bar{r})\cos\bar{\theta}]\cos(kn\bar{\theta}),$$

$$\psi_{10} = -[kn\bar{r}^{kn-1}\sin\bar{\theta}]\sin(kn\bar{\theta}) - [kn\bar{r}^{kn-1}\cos\bar{\theta}]\cos(kn\bar{\theta}),$$

$$\psi_{11} = \mathrm{ber}_0(\lambda\bar{r}),$$

$$\psi_{12} = \mathrm{bei}_0(\lambda\bar{r}),$$

$$\psi_{13} = \mathrm{ber}_{kn}(\lambda\bar{r})\cos(kn\bar{\theta}),$$

$$\psi_{14} = \mathrm{bei}_{kn}(\lambda\bar{r})\cos(kn\bar{\theta}),$$

$$\psi_{15} = \bar{r}^{kn}\cos(kn\bar{\theta}),$$

$$\psi_{16} = \left[\frac{\lambda}{\omega\bar{r}}\mathrm{bei}_0'(\lambda\bar{r}) - \frac{\nu\lambda^2}{\omega}\mathrm{bei}_0''(\lambda\bar{r})\right]\sin^2\bar{\theta} + \left[\frac{\lambda^2}{\omega}\mathrm{bei}_0''(\lambda\bar{r}) - \frac{\nu\lambda}{\omega\bar{r}}\mathrm{bei}_0'(\lambda\bar{r})\right]\cos^2\bar{\theta},$$

$$\psi_{17} = \left[-\frac{\lambda}{\omega\bar{r}}\mathrm{ber}_0'(\lambda\bar{r}) + \frac{\nu\lambda^2}{\omega}\mathrm{ber}_0''(\lambda\bar{r})\right]\sin^2\bar{\theta}$$
$$+ \left[-\frac{\lambda^2}{\omega}\mathrm{ber}_0''(\lambda\bar{r}) + \frac{\nu\lambda}{\omega\bar{r}}\mathrm{ber}_0'(\lambda\bar{r})\right]\cos^2\bar{\theta},$$

$$\psi_{18} = \left\{\left[\frac{\lambda}{\omega\bar{r}}\,\mathrm{bei}'_{kn}(\lambda\bar{r}) - \frac{1}{\omega}\left(\frac{kn}{\bar{r}}\right)^2 \mathrm{bei}_{kn}(\lambda\bar{r}) - \frac{\nu\lambda^2}{\omega}\,\mathrm{bei}''_{kn}(\lambda\bar{r})\right]\sin^2\bar{\theta}\right.$$
$$\left. + \left[-\frac{\nu\lambda}{\omega\bar{r}}\,\mathrm{bei}'_{kn}(\lambda\bar{r}) + \frac{\nu}{\omega}\left(\frac{kn}{\bar{r}}\right)^2 \mathrm{bei}_{kn}(\lambda\bar{r}) + \frac{\lambda^2}{\omega}\,\mathrm{bei}''_{kn}(\lambda\bar{r})\right]\cos^2\bar{\theta}\right\}\cos(kn\bar{\theta})$$
$$+ \left\{(1+\nu)\frac{kn}{\omega}\left[\frac{\lambda}{\bar{r}}\,\mathrm{bei}'_{kn}(\lambda\bar{r}) - \frac{1}{\bar{r}^2}\,\mathrm{bei}_{kn}(\lambda\bar{r})\right]\sin 2\bar{\theta}\right\}\sin(kn\bar{\theta}),$$

$$\psi_{19} = \left\{\left[-\frac{\lambda}{\omega\bar{r}}\,\mathrm{ber}'_{kn}(\lambda\bar{r}) + \frac{1}{\omega}\left(\frac{kn}{\bar{r}}\right)^2 \mathrm{ber}_{kn}(\lambda\bar{r}) + \frac{\nu\lambda^2}{\omega}\,\mathrm{ber}''_{kn}(\lambda\bar{r})\right]\sin^2\bar{\theta}\right.$$
$$\left. + \left[\frac{\nu\lambda}{\omega\bar{r}}\,\mathrm{ber}'_{kn}(\lambda\bar{r}) - \frac{\nu}{\omega}\left(\frac{kn}{\bar{r}}\right)^2 \mathrm{ber}_{kn}(\lambda\bar{r}) - \frac{\lambda^2}{\omega}\,\mathrm{ber}''_{kn}(\lambda\bar{r})\right]\cos^2\bar{\theta}\right\}\cos(kn\bar{\theta})$$
$$+ \left\{(1+\nu)\frac{kn}{\omega}\left[\frac{1}{\bar{r}^2}\,\mathrm{ber}_{kn}(\lambda\bar{r}) - \frac{\lambda}{\bar{r}}\,\mathrm{ber}'_{kn}(\lambda\bar{r})\right]\sin 2\bar{\theta}\right\}\sin(kn\bar{\theta}),$$

$$\psi_{20} = \frac{1+\nu}{\omega}\,kn(kn-1)\,\bar{r}^{kn-2}\{[\cos^2\bar{\theta} - \sin^2\bar{\theta}]\cos(kn\bar{\theta}) + \sin 2\bar{\theta}\sin(kn\bar{\theta})\},$$

$$\psi_{21} = \left[\lambda^2\,\mathrm{ber}''_0(\lambda\bar{r}) + \frac{\nu\lambda}{\bar{r}}\,\mathrm{ber}'_0(\lambda\bar{r})\right]\cos^2\bar{\theta} + \left[\frac{\lambda}{\bar{r}}\,\mathrm{ber}'_0(\lambda\bar{r}) + \nu\lambda^2\,\mathrm{ber}''_0(\lambda\bar{r})\right]\sin^2\bar{\theta},$$

$$\psi_{22} = \left[\lambda^2\,\mathrm{bei}''_0(\lambda\bar{r}) + \frac{\nu\lambda}{\bar{r}}\,\mathrm{bei}'_0(\lambda\bar{r})\right]\cos^2\bar{\theta} + \left[\frac{\lambda}{\bar{r}}\,\mathrm{bei}'_0(\lambda\bar{r}) + \nu\lambda^2\,\mathrm{bei}''_0(\lambda\bar{r})\right]\sin^2\bar{\theta},$$

$$\psi_{23} = \left\{\left[\lambda^2\,\mathrm{ber}''_{kn}(\lambda\bar{r}) - \nu\left(\frac{kn}{\bar{r}}\right)^2 \mathrm{ber}_{kn}(\lambda\bar{r}) + \frac{\nu\lambda}{\bar{r}}\,\mathrm{ber}'_{kn}(\lambda\bar{r})\right]\cos^2\bar{\theta}\right.$$
$$\left. + \left[-\frac{(kn)^2}{\bar{r}^2}\,\mathrm{ber}_{kn}(\lambda\bar{r}) + \frac{\lambda}{\bar{r}}\,\mathrm{ber}'_{kn}(\lambda\bar{r}) + \nu\lambda^2\,\mathrm{ber}''_{kn}(\lambda\bar{r})\right]\sin^2\bar{\theta}\right\}\cos(kn\bar{\theta})$$
$$+ \left\{\frac{kn}{\bar{r}}(1-\nu)\left[\lambda\,\mathrm{ber}'_{kn}(\lambda\bar{r}) - \frac{1}{\bar{r}}\,\mathrm{ber}_{kn}(\lambda\bar{r})\right]\sin 2\bar{\theta}\right\}\sin(kn\bar{\theta}),$$

$$\psi_{24} = \left\{\left[\lambda^2\,\mathrm{bei}''_{kn}(\lambda\bar{r}) - \nu\left(\frac{kn}{\bar{r}}\right)^2 \mathrm{bei}_{kn}(\lambda\bar{r}) + \frac{\nu\lambda}{\bar{r}}\,\mathrm{bei}'_{kn}(\lambda\bar{r})\right]\cos^2\bar{\theta}\right.$$
$$\left. + \left[-\frac{(kn)^2}{\bar{r}^2}\,\mathrm{bei}_{kn}(\lambda\bar{r}) + \frac{\lambda}{\bar{r}}\,\mathrm{bei}'_{kn}(\lambda\bar{r}) + \nu\lambda^2\,\mathrm{bei}''_{kn}(\lambda\bar{r})\right]\sin^2\bar{\theta}\right\}\cos(kn\bar{\theta})$$
$$+ \left\{\frac{kn}{\bar{r}}(1-\nu)\left[\lambda\,\mathrm{bei}'_{kn}(\lambda\bar{r}) - \frac{1}{\bar{r}}\,\mathrm{bei}_{kn}(\lambda\bar{r})\right]\sin 2\bar{\theta}\right\}\sin(kn\bar{\theta}),$$

$$\psi_{25} = kn(kn-1)(1-\nu)\,\bar{r}^{kn-2}[\sin 2\bar{\theta}\sin(kn\bar{\theta}) + (2\cos^2\bar{\theta} - 1)\cos(kn\bar{\theta})],$$

where $\bar{r}$, $\bar{\theta}$ are the coordinates of collocation points.

Substitution of the expressions for u_n and F from (3) in (4) yields the sectional resultants of stress:

$$F_{rr}(\sigma) = \frac{p_n R}{2} + A_0^1\left[\frac{\lambda}{\omega r}\mathrm{bei}_0'(\lambda r)\right] + A_0^2\left[-\frac{\lambda}{\omega r}\mathrm{ber}_0'(\lambda r)\right]$$
$$+ \sum_{n=1}^{\infty}\left\{A_{kn}^1\left[\frac{\lambda}{\omega r}\mathrm{bei}_{kn}'(\lambda r) - \frac{1}{\omega}\left(\frac{kn}{r}\right)^2\mathrm{bei}_{kn}(\lambda r)\right]\right.$$
$$+ A_{kn}^2\left[-\frac{\lambda}{\omega r}\mathrm{ber}_{kn}'(\lambda r) + \frac{1}{\omega}\left(\frac{kn}{r}\right)^2\mathrm{ber}_{kn}(\lambda r)\right]$$
$$\left. - C_{kn}^2\frac{kn(kn-1)}{\omega}r^{kn-2}\right\}\cos(kn\theta),$$

$$F_{\theta\theta}(\sigma) = \frac{p_n R}{2} + A_0^1\left[\frac{\lambda^2}{\omega}\mathrm{bei}_0''(\lambda r)\right] + A_0^2\left[-\frac{\lambda^2}{\omega}\mathrm{ber}_0''(\lambda r)\right]$$
$$+ \sum_{n=1}^{\infty}\left\{A_{kn}^1\left[\frac{\lambda^2}{\omega}\mathrm{bei}_{kn}''(\lambda r)\right] + A_{kn}^2\left[-\frac{\lambda^2}{\omega}\mathrm{ber}_{kn}''(\lambda r)\right]\right.$$
$$\left. + C_{kn}^2\left[\frac{kn}{\omega}(kn-1)r^{kn-2}\right]\right\}\cos(kn\theta),$$

$$M_{r\theta}(\sigma) = D\left[A_0^1\left[-\lambda^2\mathrm{ber}_0''(\lambda r) - \frac{\nu}{r}\lambda\,\mathrm{ber}_0'(\lambda r)\right]\right.$$
$$+ A_0^2\left[-\lambda^2\mathrm{bei}_0''(\lambda r) - \frac{\nu}{r}\lambda\,\mathrm{bei}_0'(\lambda r)\right]$$
$$+ \sum_{n=1}^{\infty}\left\{A_{kn}^1\left[-\lambda^2\mathrm{ber}_{kn}''(\lambda r) + \nu\left(\frac{kn}{r}\right)^2\mathrm{ber}_{kn}(\lambda r) - \frac{\nu}{r}\lambda\,\mathrm{ber}_{kn}'(\lambda r)\right]\right.$$
$$+ A_{kn}^2\left[-\lambda^2\mathrm{bei}_{kn}''(\lambda r) + \nu\left(\frac{kn}{r}\right)^2\mathrm{bei}_{kn}(\lambda r) - \frac{\nu}{r}\lambda\,\mathrm{bei}_{kn}'(\lambda r)\right]$$
$$\left.\left. + C_{kn}^1[-kn(kn-1)(1-\nu)r^{kn-2}]\right\}\cos(kn\theta)\right],$$

$$M_{\theta r}(\sigma) = D\left[A_0^1\left[\frac{\lambda}{r}\mathrm{ber}_0'(\lambda r) + \nu\lambda^2\mathrm{ber}_0''(\lambda r)\right] + A_0^2\left[\frac{\lambda}{r}\mathrm{bei}_0'(\lambda r) + \nu\lambda^2\mathrm{bei}_0''(\lambda r)\right]\right.$$
$$+ \sum_{n=1}^{\infty}\left\{A_{kn}^1\left[-\left(\frac{kn}{r}\right)^2\mathrm{ber}_{kn}(\lambda r) + \frac{\lambda}{r}\mathrm{ber}_{kn}'(\lambda r) + \nu\lambda^2\mathrm{ber}_{kn}''(\lambda r)\right]\right.$$
$$+ A_{kn}^2\left[-\left(\frac{kn}{r}\right)^2\mathrm{bei}_{kn}(\lambda r) + \frac{\lambda}{r}\mathrm{bei}_{kn}'(\lambda r) + \nu\lambda^2\mathrm{bei}_{kn}''(\lambda r)\right]$$
$$\left.\left. + C_{kn}^1[-kn(kn-1)(1-\nu)r^{kn-2}]\right\}\cos(kn\theta)\right].$$

First derivatives of KELVIN functions of kn-th order with respect to λr can be expressed by:

$$\mathrm{ber}'_{kn}(\lambda r) = -\frac{1}{\sqrt{2}}[\mathrm{ber}_{kn-1}(\lambda r) + \mathrm{bei}_{kn-1}(\lambda r)] - [k n \,\mathrm{ber}_{kn}(\lambda r)],$$

$$\mathrm{bei}'_{kn}(\lambda r) = \frac{1}{\sqrt{2}}[\mathrm{ber}_{kn-1}(\lambda r) - \mathrm{bei}_{kn-1}(\lambda r)] - [k n \,\mathrm{bei}_{kn}(\lambda r)].$$

Second derivatives of KELVIN functions of kn-th order with respect to λr can be expressed by:

$$\mathrm{ber}''_{kn}(\lambda r) = -\frac{1}{\lambda r}\mathrm{ber}'_{kn}(\lambda r) + \left(\frac{k n}{\lambda r}\right)^2 \mathrm{ber}_{kn}(\lambda r) - \mathrm{bei}_{kn}(\lambda r),$$

$$\mathrm{bei}''_{kn}(\lambda r) = -\frac{1}{\lambda r}\mathrm{bei}'_{kn}(\lambda r) + \left(\frac{k n}{\lambda r}\right)^2 \mathrm{bei}_{kn}(\lambda r) + \mathrm{ber}_{kn}(\lambda r).$$

Bibliography

1. G. A. ORAVAS: "Stress and Strain in Thin Shallow Spherical Calotte Shells". International Association for Bridge and Structural Engineering, Zurich, v. 17, 1957, p. 139.
2. F. TÖLKE: «Über Spannungszustände in dünnen Rechteckplatten». Ingenieur-Archiv, v. 5, 1934, p. 187.
3. A. H. MUSHTARI: «Nekotorye obobshcheniya teorii tonkikh obolochek». Izvestiya Fiziko-Matematicheskogo obshchestva pri Kazanskom Universitete, v. 11, series 8, 1938.
4. V. Z. VLASOV: «Obshchaya teoriya obolochek i ee prilosheniya v tekhnike». Gostekhizdat, Moscow, 1949, p. 295. (NASA Technical Translation TT F-99, April 1964.)
5. K. MARGUERRE: «Zur Theorie der gekrümmten Platte großer Formänderung». Proc. 5th International Congress of Applied Mechanics. Cambridge, Mass., J. Wiley, New York, 1939.
6. D. S. WALKINSHAW: "On Thin Shallow Elastic Shells over Polygonal Bases". Thesis, McMaster University, Canada, 1965.
7. G. E. RILEY: "Stress and Strain in a Shallow Elastic Calotte Shell". Thesis, McMaster University, Canada, 1964.

Summary

An approximate solution is presented for the flexure of thin spherical shells of polygonal plan in which edge conditions are satisfied exactly only at discrete collocation points on the shell's boundary. Sectional resultants obtained both theoretically and experimentally for a spherical shell over an hexagonal base and theoretically for a shell over a triangular base are graphically depicted for various radial lines on the characteristic segment of each shell.

Résumé

On présente une solution approchée pour le calcul de la flexion des coques minces sphériques à base polygonale, pour lesquelles les conditions aux limites sont exactement remplies seulement en certains points du bord de la coque. On a représenté graphiquement pour différentes radiales, d'une part les efforts obtenus théoriquement et expérimentalement pour une coque sphérique à base hexagonale et, d'autre part, ceux obtenus théoriquement pour une coque à base triangulaire.

Zusammenfassung

Dargestellt wird eine Näherungslösung für die Biegung dünner Kugelschalen vieleckigen Grundrisses, deren Kantenbedingungen nur in bestimmten Punkten der Schalenränder genau erfüllt sind. Die Spannungen, für eine Schale über sechseckigem Grundriß theoretisch wie experimentell und für eine solche über dreieckigem Grundriß theoretisch erhalten, werden für verschiedene Öffnungswinkel in ausgewählten Schnitten zeichnerisch dargestellt.